- Technical Paper -

EFFECT OF CONCRETE FLOW ON THE FLEXURAL BEHAVIOR OF FIBER REINFORCED SELF-COMPACTING CONCRETE BEAMS

Ramiz A. RAJU [*1], Sopokhem LIM[*2], Takumi KAGEYAMA[*3] and Mitsuyoshi AKIYAMA[*4]

ABSTRACT

The effectiveness of steel fibers in reinforcing concrete beams depends on whether a uniform distribution of fibers parallel to the axis is achieved. However, placing and compacting steel fiber reinforced concrete (SFRC) into a specimen mold by vibration can negatively affect the fiber distribution and orientation, and eventually its structural performance. This paper presents an effort for improving the structural performance of SFRC members by manipulating the high-flowability and self-placability properties of self-compacting concrete to achieve better distribution and orientation of fibers.
Keywords: self-compacting concrete, fiber distribution, fiber orientation, X-ray image, concrete flow

1. INTRODUCTION

The effectiveness of steel fibers in reinforcing concrete members primarily relies on achieving a uniform distribution of fibers which are oriented in a direction countering the external stress. To improve the flexural performance of steel fiber reinforced concrete (SFRC) members, one might consider to increase the fiber contents to make the SFRC more homogenous. However, previous experimental researches [1,2] have demonstrated that the distribution of fibers in concrete structures is hardly uniform due to the effects of many parameters (e.g., vibration, boundary forms, placing methods, and properties of steel fibers) during the fabrication process. Consequently, increasing fiber content does not always lead to higher flexural performance of SFRC beams [3,4]. The use of self-compacting concrete (SCC) instead of normal concrete can be a good solution to reduce the fiber segregation since SCC is a high-performance material which is able to flow and fill a mold under its own weight without the need of vibration [5-8].

Recently, efforts have been made to improve the structural performance of SFRC beams by manipulating the high-flow properties of self-compacting concrete to align the fibers in a favorable direction and achieve more uniform distribution of steel fibers. Stähli et al. [9] investigated the effect of different flow velocities of self-compacting concrete on the orientation and distribution of fibers in small prisms (70 mm × 70 mm × 280 mm) cut from a U-shape specimen. Using the X-ray tomography, these authors found the fibers aligned with the flow of concrete and higher flow led to better alignment of fibers and higher flexural performance. Torrijos et al. [10] examined the effect of three different concrete casting methods on the fiber distribution and flexural performance of self-compacting steel fiber

reinforced concrete (SCFRC) prisms (150 mm × 150 mm × 280 mm): (a) from the vertical direction of the mold, (b) from the center of the mold, and (c) through a tube by flowing the concrete from one side to another. It was reported that the third casting method (c) provided highest flexural responses than the other two methods due to better alignment of fibers to the flow of concrete. Vandewalle et al. [11] investigated the effect of the flow distance and types of concrete (self-compacting and normal concrete) on the flexural performance of the prisms (150 mm × 150 mm × 600 mm) that cut from a long beam. After checking the fiber distribution by X-ray images and fiber counting at the cracked cross-section, they found that fibers aligned to the flow, however beyond a certain distance, their alignment did not increase with the flow distance anymore. Furthermore, the better alignment of fibers in the direction of SCFRC generates higher peak loads and better post-cracking performance compared to the SFRC [12,13].

This paper presents an effort for improving the structural performance of SFRC members by manipulating the high-flowability and self-placability properties of self-compacting concrete to achieve better distribution and orientation of fibers. Effects of flow distance of self-compacting concrete and types of concrete (i.e., self-compaction versus normal concrete) on their different structural performance associated with distribution and orientation are investigated. The outcomes of this research aim at achieving a reliable method to reproduce the precast SFRC beams with a reduced scattering structural performance due to fiber dispersion.

2. EXPERIMENTAL PROGRAMS

2.1 Test Materials

The quality of materials which were used in the

---

*1   Graduate School of Creative Sciences and Engineering, Waseda University, JCI Student Member
*2   Graduate School of Creative Sciences and Engineering, Waseda University, JCI Student Member
*3   Graduate School of Creative Sciences and Engineering, Waseda University
*4   Professor, Dept. of Civil and Environmental Engineering, Waseda University, JCI member

experiment is given as follows. The coarse aggregates (C.A.) used in this study has a maximum size of 20 mm and a specific density of 2.64 g/cm^3. The fine aggregate (F.A.) has a specific density of 2.60 g/cm^3 and a fineness modulus of 2.64 g/cm^3. The local limestone (L.S.) filler, namely Industrial Tankar-325, was used as partial replacement of the cement amount for the economical purpose to produce SCFRC. A water reducing superplasticizer was utilized in order to produce a high-flowability and high-workability concrete. In addition, an air entraining (A.E.) admixture was added to improve the stability of air-entrainment of the concrete mix. A doubled hooked-end steel fiber was used for this study (see the details of fiber properties in Table 1).

2.2 Mix Proportion

According to the research objective, two different types of concrete, SCFRC and SFRC, were designed. For SCFRC, the mixing proportion was determined by performing several trial mixes. Slump flow (over 650 mm), compressive strength (about 50 MPa), and very low segregation and bleeding were the main criteria for determining the mix design of SCFRC. According to [14], the required slump value shall range from 650 to 800 mm in order to flow the concrete in the horizontal direction. As a result of trial mixes, the concrete mixing proportions are selected as listed in Table 2. The average diameters of slump flow test for SCFRC-1 and SCFRC-2 are 740 mm and 699 mm, respectively, while the height of slump cone test for SFRC is 2 cm. The 28-day compressive strength was 48 MPa, 52 MPa, and 42 MPa for SCFRC-1, SCFRC-2, and SFRC-1, respectively.

Table 1 Characteristics of steel fiber

Shape	Length	Dia.	Aspect ratio	Tensile strength
	(mm)	(mm)		(MPa)
	60	0.9	65	2300

Table 2 Mixing proportions of concrete

Mix	SCFRC-1	SCFRC-2	SFRC-1
	(kg/m³)	(kg/m³)	(kg/m³)
Water	175	175	175
Cement	318	318	350
L.S.	224	224	-
F.A.	1006	1006	950
C.A.	552	552	789
Steel Fiber	20	40	40
Plasticizer	4.29	4.61	3.50
A.E.	0.64	0.64	0.70

2.3 Experimental Procedure

The experimental program is established to investigate (a) the influence of the flow behavior of SCFRC on the fiber distribution and orientation and (b) the different flexural behavior of SCFRC versus SFRC beams. Table 3 shows the details of the specimens used in this experiment.

To investigate the flow behavior of SCFRC, 1900-mm-long beams were fabricated using two different fiber contents, 20 kg/m^3 and 40 kg/m^3 for the
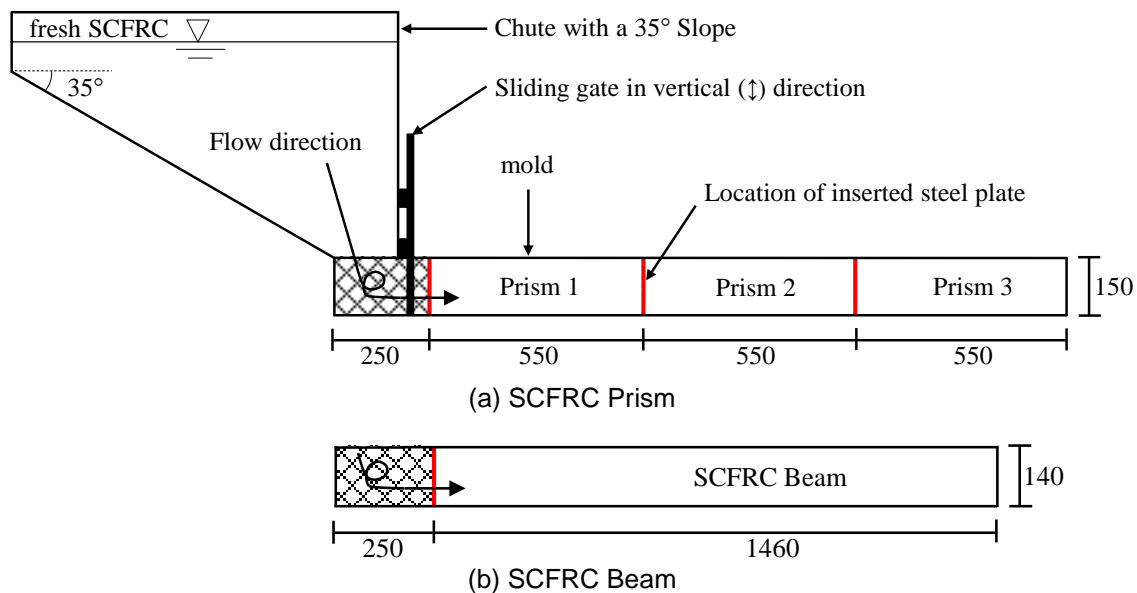

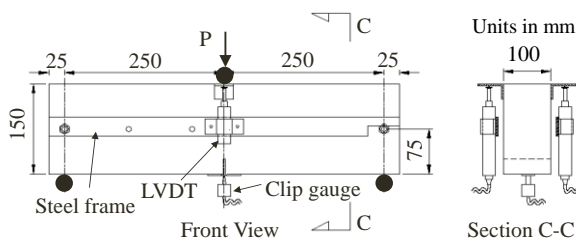Fig.1 Mold setup for SCFRC and SCFRC specimens
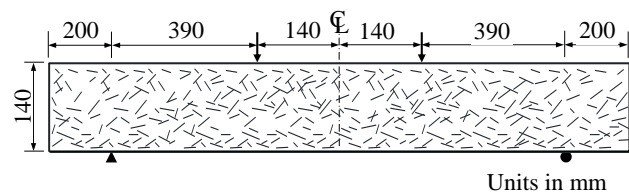

Fig.2 Bending test setup of the prism

Fig.3 Bending test setup of the beam

Table 3 Details of the test specimen

Specimen	Notation	#	Cross-Section (mm^2)	Length (mm)	Mix Proportion
Prism	PS20	3	100 × 150	550	SCFRC-1
	PS40	3	100 × 150	550	SCFRC-2
	PN40	6	100 × 150	550	SFRC-1
Beam	BS20	1	100 × 140	1460	SCFRC-1
	BS40	1	100 × 140	1460	SCFRC-2
	BN40	1	100 × 140	1460	SFRC-1

prism series PS20 and PS40, respectively. Fig. 1(a) illustrates the mold setup for the concrete casting of SCFRC prisms. The design concept of the mold setup was inspired from Vandewalle et al. [11]. A home-made chute with a 35-degree slope was designed as a stand-alone container which is used to retain a sufficient amount of concrete for filling a specimen mold completely. Before the concrete casting, a specimen mold was placed under the chute's outlet; and then a sliding door was pushed down to close the opening. During concrete casting, the chute was used to temporarily store the concrete. Once the sliding gate was lifted up, the concrete can be flowed and fill the mold completely. Soon after the casting, the beam was divided into three prisms by inserting three steel plates at different locations as shown in Fig. 1(a). The three prisms were labeled as prism 1, prism 2, and prism 3, respectively, from the casting point. Then, a notch at the middle of each prism was made by inserting an aluminate plate (3 mm × 25 mm × 100 mm) from the bottom of the specimens through hollow channels.

To investigate the structural behavior of SCFRC, two beams using self-compacting concrete (i.e., BS20 and BS40 with fibers 20 kg/m^3 and 40 kg/m^3) were tested. The beams were fabricated following the same procedure for making the SCFRC prism. Fig. 1(b) shows the mold used for BS20 and BS40. The first 250 mm of all SCFRC beams (hatched section in Figs. 1(a) and 1(b)) was not used for any testing. Since a turbulent flow is expected at the casting point, the fiber directions are completely random and unpredictable.
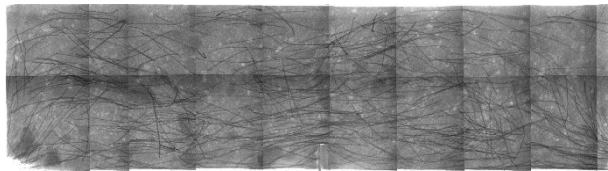
Finally, in order to compare the fiber dispersion properties (i.e. fiber distribution and orientation) and flexural performance between SCFRC and SFRC, one series of 6 prisms (100 mm × 150 mm × 550 mm) and a
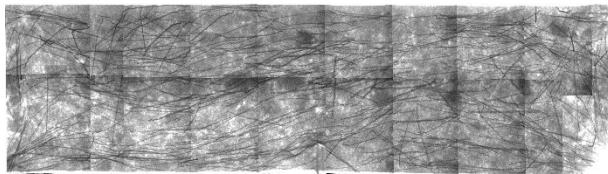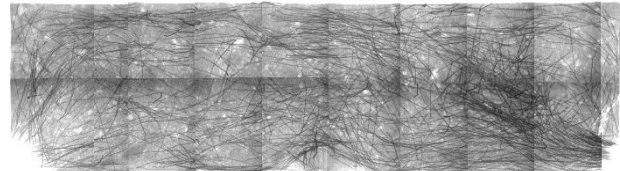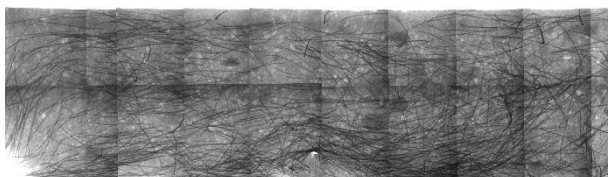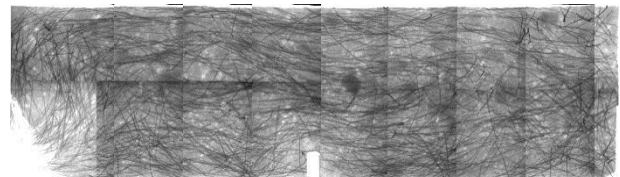

(a) PS20-1
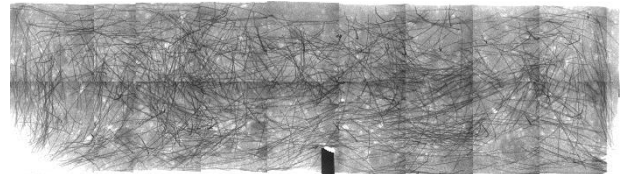
(b) PS20-2

(c) PS20-3

Fig.4 X-ray image of PS20 prism series

(a) PS40-1

(b) PS40-2

(c) PS40-3

Fig.6 X-ray image of PS40 prism series
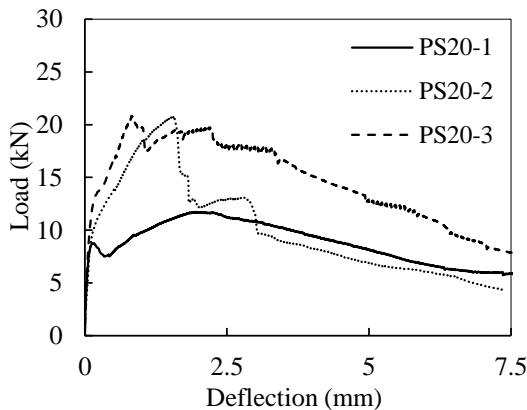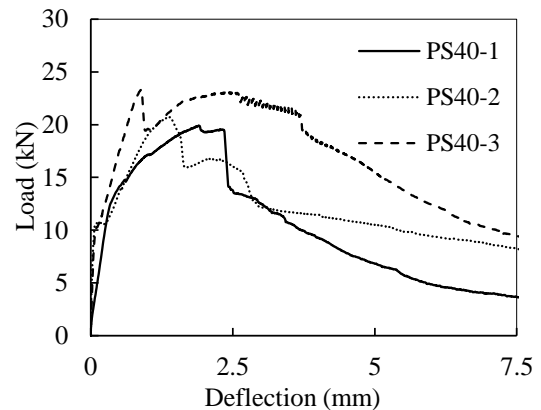

Fig.5 P-δ response of the PS20 prism series

Fig.7 P-δ response of the PS40 prism series

beam (100 mm × 140 mm × 1460 mm) were fabricated using normal concrete and a fiber content of 40 kg/m³. The molds shown in Fig. 1 were not used due to the absence of self-consolidation properties in normal concrete. The specimens are fabricated according to the casting method in [15]. In the procedure, the casting of the prism and beam were started by pouring the concrete in the middle part and followed by both ends of the specimens. The compaction was carried out by external vibration in order to prevent the direct contact with fibers.

Two days after casting the concrete, the molds of all specimens were removed. Next, seven days after casting, X-ray photography was performed on the lateral side of all specimens using the X-ray machine at the Material Engineering laboratory, Waseda University. At the 28th day, three-point bending test of prisms was performed as shown in Fig. 2. Compression and splitting tests of cylinders were performed to obtain the compressive strength and tensile strength, respectively. Finally, the four-point bending test of the SCFRC and SFRC beams were conducted (see Fig. 3).

3. TEST RESULTS AND DISCUSSIONS

3.1 Effects of Concrete Flow on Fiber Distribution and Orientation

Fig. 4 shows the X-ray images (550 mm × 150 mm) of each prism in series PS20, which contains 20 kg/m³ of fiber. From the X-ray images, it can be seen that the distribution of the fibers is quite uniform within the cross-section of individual prisms. Although the concentration of the fibers is relatively higher at the bottom of the prism due to the settlement, the orientation of the fibers in all prism is parallel to the flow direction of the concrete. By comparing Figs. 4(a), 4(b), and 4(c), it can be seen that the distribution of fibers over the length of the beam is not the same. PS20-3 contains the highest amount of fibers followed by PS20-2 and PS20-1, respectively. This trend means that the further the flow distance, the greater the fiber amount. This behavior might be attributed to two factors. The first factor is that more fibers had already settled down to the bottom of the chute within the period for filling SCFRC before the discharge of concrete. The second one is highest flow velocity at the opening of the sliding gate which occurred due to the sudden pressure, at the instant the sliding gate was lifted up. These combined factors brought the fibers to the end of the flow. As a result, the fiber distribution associated with the flow behavior yields the load-deflection (P-δ) relationship of the prisms as shown in Fig. 5, where the PS20-3 exhibits highest post-cracking performance compared to PS20-1 and PS20-2. Although PS20-2 displays similar peak load to PS20-3, it provided lower energy absorption capacity since it had only fewer fibers in PS20-2.

Fig. 6 depicts the flow behavior from the X-ray images (550 mm × 150 mm) of the prism series PS40. Similar to flow behavior of prism series PS20, most of the fibers were transported through the high flow of concrete to the last prism PS40-3. Therefore, PS40-3 had the most fibers, compared to the other two prisms, PS40-1 and PS40-2. On the contrary, different from the flow
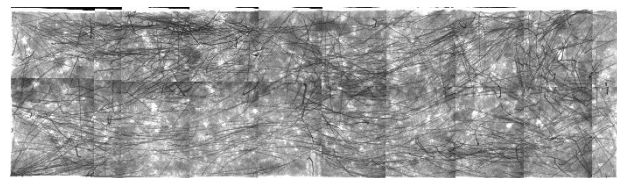
(a) PN40-1
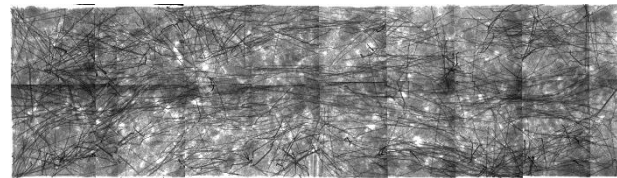
(b) PN40-4

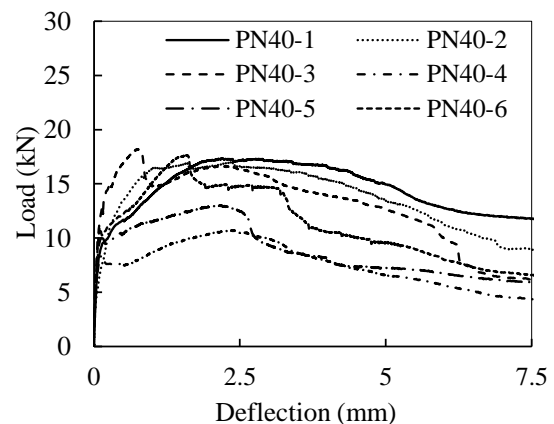Fig.8 X-ray image of PN40 prism series

Fig.9 P-δ response of the PN40 prism series

behavior of prism series PS20, PS40-1 has more fibers yet poorer alignment than PS20-1 (see Fig. 6(a) and Fig. 5(a)). The reason behind this behavior might be the increased fiber content in prism series PS40 compared to PS20. This caused a congestion of fibers in the first prism PS40-1 as flow velocity subsided due to less amount of concrete remaining in the chute. Nonetheless, the orientation of fibers in PS40-2 and PS40-3 became better due to the higher flow of concrete. It can be said that the higher flow induced better alignment of fibers to the flow direction. As a result, PS40-3 with the most fibers displays the highest post-cracking performance in the series (see Fig. 7).

Through observation of the outcomes from the prism series PS20 and PS40, it is evident that the fibers in the farthest part of the beam from the point of casting, consists of the maximum amount and best alignment of fibers and thus gives a superior post-cracking performance.

Note that at ends of the beam, some vertically positioned fibers were observed due to the resistance from the wall of the specimen mold and the steel plates which were inserted in the mold to divide the beam into small prisms soon after casting the concrete. However, these fibers cannot contribute to the betterment of the mechanical behavior of the prisms since their locations were out of the effective span during the test.
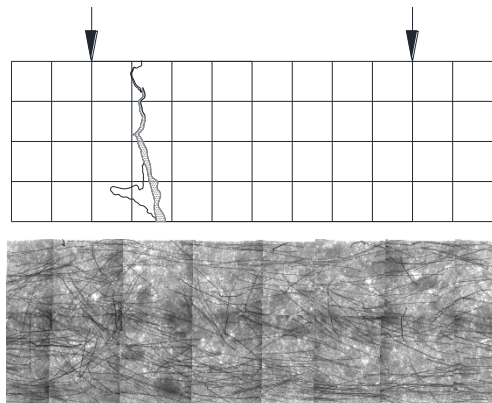
Fig. 8 and Fig. 9 show the X-ray images (550 mm × 150 mm) and P-δ responses, respectively, of normal kg/m³. From the X-ray images, it can be seen that the
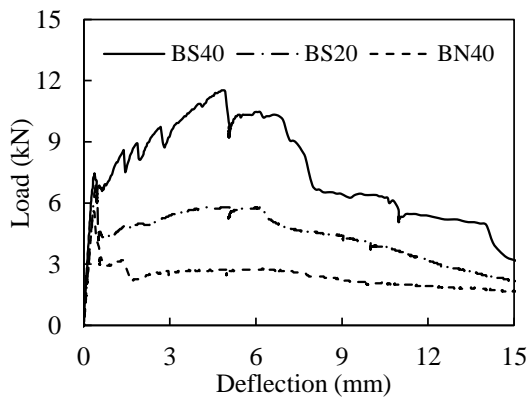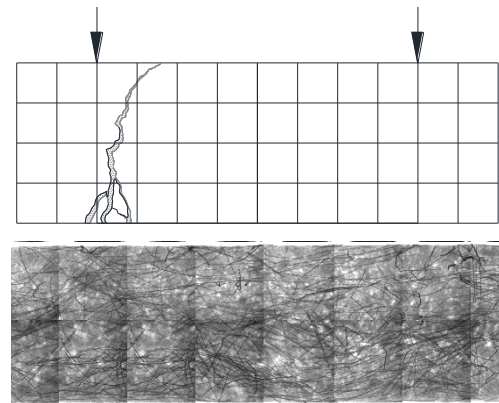
(a) P-δ responses of SCFRC beams
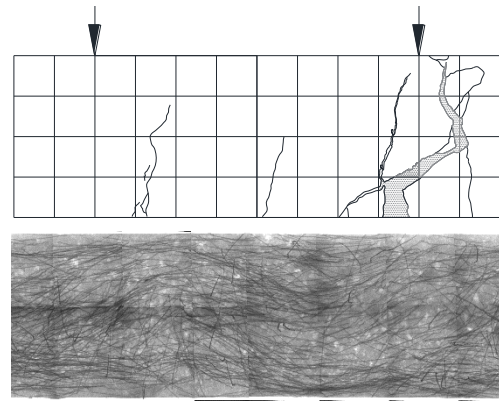
(b) BS40

(c) BS20

(d) BN40

Fig.10 Real crack location compared with X-ray image and P-δ response of BS40, BS20, and BN40

distribution of fibers is highly random and scattered although they have the same amount of steel fibers. Consequently, a large scatter of post-cracking P-δ responses can be noticed.

From the comparison of Fig. 7 and Fig. 9, it can be observed that PS40 provides better and less scattered post-cracking performance in comparison to PN40 due to the better orientation and more uniform distribution of fibers which are affected by the flow.

3.2 Flexural Performance and Crack Behavior of SCFRC and SFRC Beams

Fig. 10(a) shows the flexural behavior of beams BS20, BS40, and BN40. Figs. 10(b), 10(c) and 10(d) depict the X-ray images (420 mm × 140 mm) and the cracking behavior of the beams BS40, BS20, and BN40, respectively. From the test results, as expected, the flexural performance of BS40 is better than that of BS20 since BS40 contains more fibers than BS20. In addition, from Fig. 10(a) and Table 4, it is worth noting that the loading capacity and energy absorption of BS40 are 11.52 KN and 144.34 kN.mm which are 2 times and 3 times as large as the loading capacity and energy absorption of BN40, respectively. This is due to the better orientation and more uniform distribution of fibers of BS40 compared to those of BN40 (see X-ray images in Figs. 10(b) and 10(d).

The most interesting result is that, even if the beam BS20 contains lower fiber amount than BN40, the flexural behavior of BS20 is higher. More precisely, the energy absorption capacity of BS20 is twice compared

Table 4 Peak load and area under the P-δ curve of SCFRC and SFRC beams

SCFRC Beam	Peak Load (kN)	Area under the curve (kN.mm)
BS40	11.52	144.3
BS20	6.86	78.6
BN40	5.59	39.4

to BN40. This is a strong indication that the mechanical behavior of the SCFRC and SFRC beams depends much on fiber distribution and orientation. SCFRC is superior in mechanical performance.

Figs. 10(b), 10(c), and 10(d) depict the crack patterns within the constant moment region of all beams. It can be detected from Figs. 10(c) and 10(d) that only one primary crack occurred in BS20 and BN40. The reason might be that the cracks only occurred at the weakest point of the beam where the amount of fiber is low or the orientation of the fibers is not well aligned. On the contrary, one primary crack can be spotted along with multiple secondary cracks for the beam BS40. From the X-ray image, it can be distinguished that the fiber alignments are much better in BS40 comparing with BN40. Multiple cracks appeared as a consequence of the loading due to more uniform tensile stress distribution in the beam [16].

4. CONCLUSIONS

In this paper, the experimental program has been conducted to observe the distribution and orientation of

fiber due to SCFRC flow behavior using X-ray image and to investigate the mechanical behavior of SCFRC and SFRC beams.

The following conclusions were drawn:
(1) The distribution of fibers is more uniform in SCFRC than that of SFRC due to the self-consolidating properties and no use of vibration.
(2) The orientation of fiber is better for the SCFRC due to the higher flow of the concrete.
(3) The post-cracking performance for SCFRC members is superior to the SFRC ones due to the better alignment of the fibers.
(4) For the flexural performance of the beams, the loading capacity and energy absorption of BS40 are greater than those of BN40 by 2 and 3 times, respectively. In addition, BS20 has a better perform in energy absorption capacity than BN40 by 2 times due to the uniform distribution and better orientation of fibers even though the amount of fiber in BS20 is half of BN40.

From the outcome of this experimental research, it can be seen that it is difficult to achieve the uniform distribution and good orientation of fibers over the entire beam even using the self-compacting concrete. This posts a problem since the flexural bending capacity of a SCFRC beam is not constant over its length but significantly depends on the localization of a weak part of the beam which has poor fiber distribution and orientation. Further research is needed to identify the optimal casting method to obtain uniform distribution of fiber over the beam. This can be established by investigating the effect of different slump flow in order to achieve the optimal casting flow. In addition, future research should be conducted to observe the effect of different fiber amount (other than 20 kg/m^3 and 40 kg/m^3) on SCC flow.

REFERENCES

[1] Edgington, J. and Hannant, D. J., "Steel Fiber Reinforced Concrete. The Effect on Fiber Orientation of Compaction by Vibration," Materials and Structure, Vol. 5, 1972, pp. 41-44.

[2] Abrishambaf, A., Barros, A. O. and Cunha, V. M. C. F., "Relation Between Fibre Distribution and Post-Cracking Behaviour in Steel Fibre Reinforced Self-Compacting Concrete Panels," Cement and Concrete Research, Vol. 51, 2013, pp. 57-66.

[3] Lim, S., Matsuda, M., Raju, R. A. and Akiyama, M., "Flexural Behavior Prediction of SFRC Beams using Finite Element Method and X-ray Image," JCI Annual Convention, Vol. 39(2), 2017, pp. 1099-1104.

[4] Lim, S., Okamoto, T., Matsuda, M. and Akiyama, M., "Flexural Behavior Prediction of SFRC Beam: A Novel X-Ray Technique," JCI Annual Convention, Vol. 38(2), 2016, pp. 1351-1356.

[5] Ye, G., Liu, X., Schutter, G. De, Poppe, A. –M. and Taerwe L., "Influence of Limestone Powder used as Filler in SCC on Hydration and Microstructure of Cement Pastes," Cement & Concrete Composites, Vol. 26, 2007, pp. 94-102.

[6] Zhu, W. and Gibbs, J. C., "Use of Different Limestone and Chalk Powders in Self-Compacting Concrete," Cement and Concrete Research, Vol. 35, 2005, pp. 1457-1462.

[7] Ghezal, A. and Khayat, K. H., "Optimizing Self-Consolidating Concrete With Limestone Filler by using Statistical Factorial Design Methods," ACI Materials Journal, Vol. 99(3), 2002, pp. 264-272.

[8] Yahiaa, A., Tanimurab, M. and Shimoyama Y., "Rheological Properties of Highly Flowable Mortar Containing Limestone Filler-effect of Powder Content and W/C Ratio," Cement and Concrete Research, Vol. 35, 2005, pp. 532-539.

[9] Stähli, P., Custer, R. and Mier J. G. K. van, "On Flow Properties, Fibre Distribution, Fibre Orientation and Flexural Behaviour of FRC," Materials and Structures, Vol. 41, 2008, pp. 189-196.

[10] Torrijos, M. C., Barragan, B. E. and Zerbino, R. L., "Placing Conditions, Mesostructural Characteristics and Post-Cracking Response of Fibre Reinforced Self-Compacting Concretes," Construction and Building Materials, Vol. 24, 2010, pp. 1078-1085.

[11] Vandewalle, L., Heirman, G. and Rickstal, F. V., "Fibre Orientation in Self-compacting Fibre Reinforced Concrete," 7th Int. RILEM Symp., 2008, pp. 719-728.

[12] Grünewald, S., "Performance-Based Design of Self-compacting Fibre Reinforced Concrete," Doctor Thesis, Delft University of Technology, 2004, pp. 147-164.

[13] Akcay, B. and Tasdemir, M. A., "Mechanical Behaviour and Fibre Dispersion of Hybrid Steel Fibre Reinforced Self-compacting Concrete," Construction and Building Materials, Vol. 28, 2012, pp. 287-293.

[14] EFNARC, The European Guidelines for Self-Compacting Concrete: Specification, Production and Use, May 2005.

[15] RILEM TC 162-TDF, "Test and Design Method for Steel Fiber Reinforced Concrete. Bending Test, Final Recommendation," Materials and Structures, Vol. 35, 2002, pp. 579-582.

[16] Ding, Y., Zhang, Y. and Thomas, A., "The Investigation on Strength and Flexural Toughness of Fibre Cocktail Reinforced Self-Compacting High Performance Concrete," Construction and Building Materials, Vol. 23, 2009, pp. 448-452.